Throughput Modeling and Validations for MIMO-OTA Testing with Arbitrary Multipath

Chen, Xiaoming; Fan, Wei; Hentilä, Lassi; Kyösti, Pekka; Pedersen, Gert F.

Published in:
I E E E Antennas and Wireless Propagation Letters

DOI (link to publication from Publisher):
10.1109/LAWP.2018.2808357

Publication date:
2018

Document Version
Early version, also known as pre-print

Throughput Modeling and Validations for MIMO-OTA Testing with Arbitrary Multipath

Xiaoming Chen, Wei Fan, Lassi Hentilä, Pekka Kyösti, and Gert F. Pedersen

Abstract—**A simple throughput model for multiple-input multiple-output (MIMO) systems has been proposed in the literature. The model takes the MIMO antenna effects into account and shows good agreement with measured throughputs in a reverberation chamber (RC). The RC emulates a multipath environment with isotropic incoming angular distribution and Rayleigh (or Rician) fading channel. In this work, we extend the throughput model to arbitrary multipath environments and verify it using (synthesized) multi-probe anechoic chamber method and two-stage method with various channel models. The throughput model can well predict the measured throughputs of all the cases.**

***Index Terms*—Multiple-input multiple-output (MIMO), over-the-air (OTA) testing, throughput modeling**

I. Introduction

Multiple-input multiple-output (MIMO) techniques have been used ubiquitously in modern communication systems such as long term evolution (LTE). Therefore, there is a strong need for efficient testing of the throughput performance of a MIMO terminal [1]. Throughput measurements of LTE terminals have been reported using various MIMO over-the-air (OTA) testing methods [2]-[6]. Tremendous effort is ongoing in the 3rd generation partnership project (3GPP) standardization on MIMO-OTA harmonization, where the objective is to ensure same throughput results should be achieved with the same MIMO-OTA method in different laboratories (i.e. inter-lab campaign) and same throughput results with different MIMO-OTA methods (i.e., inter-technique campaign) [7]. However, the progress has been slow due to measurement uncertainties in the practical testing systems and the lack of a reference throughput model. Comparisons of different MIMO-OTA testing methods are out of the scope of this study. Instead, we focus on throughput modeling that will facilitate the MIMO-OTA harmonization.

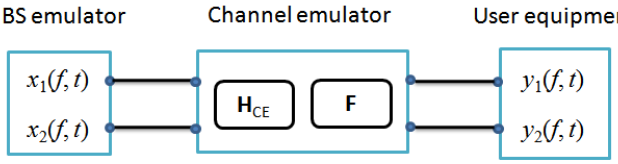

Fig. 1. Measurement setup for 2×2 MIMO throughput testing.

X. Chen is with the School of Electronic and Information Engineering, Xi'an Jiaotong University, Xi'an 710049, China (email: xiaoming.chen@mail.xjtu.edu.cn). W. Fan and G. F. Pedersen are with the Antennas, Propagation and Radio Networking section at the Department of Electronic Systems, Aalborg University, Aalborg 9000, Denmark (email: wfa@es.aau.dk). P. Kyösti and L. Hentilä are with Keysight Technologies Finland Oy, Oulu 90590, Finland. This work was partially supported by the Danish council for independent research (grant number: DFF611100525). (Corresponding author: Wei Fan.)

A simple throughput model has been proposed in [5] for single-input multiple-output (SIMO) systems and, later on, extended to MIMO system in [6]. The model shows good agreement with LTE throughput measurements in a reverberation chamber (RC). The RC emulates multipath environments with isotropic angular distribution and Rayleigh (or Rician) fading channels [8]-[10]. Hence, the previous throughput model is limited to the Kronecker channel model [11] with isotropic angular distribution and complex Gaussian channel coefficients (e.g., reverberation chambers). In this work, we extend the throughput model to arbitrary multipath environments with arbitrary channel distribution and angular power spectrum so that it is applicable to the two-stage method [4], [12] and the multi-probe anechoic chamber (MPAC) method [2], [13]. In order to verify the extended throughput model, the downlink signals generated by the BS emulator are sent conductively to the input ports of the channel emulator, where the signals are convolved with multipath fading channels. The output ports of the channel emulator are connected to the antenna ports of a mobile phone conductively via radio frequency (RF) cables (see Fig. 1). Strictly speaking, the measurement setup is for the two-stage method (where the measured antenna patterns are imported into the channel emulator). Nevertheless, it is shown the MPAC method can be synthesized by importing the measured channels in the MPAC ($\mathbf{F}$) and antenna patterns into the channel emulator [13] (see also Section III). It is shown that the throughput model can well predict the throughput measurements with various channel models for both the two-stage method and the synthesized MPAC method (cf. Section III). To the best knowledge of the authors, there are no such simple yet accurate throughput models for the MPAC and two-stage methods in the previous literature. The throughput model can be used to double check the measurement results and to complement experimental studies (e.g., with arbitrary antenna effects) for the MPAC and two-stage methods, making it easier to identify systematic errors in MIMO-OTA testing. Thus, it shows great potential of being a reference model that can be used to facilitate the MIMO-OTA harmonization in the 3GPP standardization.

Notations: Throughout this letter, *, ^{T}, and ^{H} denote complex conjugate, transpose, and Hermitian, respectively. Lowercase bold letter ($\mathbf{x}$) and uppercase bold letter ($\mathbf{X}$) represent column vector and matrix, respectively. $\|\mathbf{x}\|$ denotes the 2-norm of $\mathbf{x}$. $[\mathbf{X}]_{i,i}$ denotes the ith diagonal element of $\mathbf{X}$. E denotes the expectation. $\mathbf{I}$ represents the identity matrix.

II. THROUGHPUT MODELS

For a given modulation and coding scheme, the LTE throughput can be modeled as [5], [14]

$$T_{\text{put}}(\bar{\gamma}) = T_{\text{put,max}}\left(1 - F(\gamma_{th};\bar{\gamma})\right) \quad (1)$$

where $\bar{\gamma}$ is the average signal-to-noise ratio (SNR), γ_{th} is the threshold value, F is the cumulative distribution function (CDF) of the instantaneous SNR, $T_{\text{put,max}}$ is the maximum throughput. The analytical expression of $F(\gamma_{th};\bar{\gamma})$ is generally unknown, except for the special case of narrowband Rayleigh-fading MIMO channel with zero-forcing (ZF) receiver [6]. As a result, we use the empirical CDF to approximate it.

In the previous throughput modeling work [6], the MIMO channel is modeled by the Kronecker model as $\mathbf{R}_r^{1/2}\mathbf{H}_w\mathbf{R}_t^{1/2}$, where the MIMO channel matrix $\mathbf{H}_w$ contains independent and identically distributed (i.i.d.) complex Gaussian elements, the matrix $\mathbf{R}_t$ and the matrix $\mathbf{R}_r$ are the correlation matrices at the transmit and receive sides, respectively. The throughput model has only been validated by throughput measurements in an RC [5], [6]. In this work, we extend the throughput model to arbitrary multipath environments and validate the model using arbitrary multipath fading channels. Specifically, the spatial channel model extended (SCME) urban micro (UMi) and urban macro (UMa) tap delay line (TDL) models [15] are chosen for the validation, because they have been selected as standardized channel models for MIMO-OTA testing [1].

The MIMO channel at the kth subcarrier of the orthogonal frequency division multiplexing (OFDM) can be modeled as

$$\mathbf{y}_k = \mathbf{H}_k\mathbf{x}_k + \mathbf{n}_k \quad (2)$$

where $\mathbf{H}_k$ is an $N_R \times N_T$ MIMO channel matrix (with N_T and N_R denoting the numbers of transmit and receive antennas, respectively), $\mathbf{x}_k$ and $\mathbf{y}_k$ are $N_T \times 1$ transmit and $N_R \times 1$ receive signal vectors, respectively, and $\mathbf{n}_k$ is an $N_R \times 1$ noise vector with i.i.d. Gaussian elements, all at the kth subcarrier. The instantaneous SNR at the kth subcarrier after the minimum mean square error (MMSE) decoder is [11]

$$\gamma_i^{(k)} = \frac{1}{\left[\left(\bar{\gamma}_0\mathbf{H}_k^H\mathbf{H}_k + \mathbf{I}\right)^{-1}\right]_{i,i}} - 1 \quad (3)$$

where $\bar{\gamma}_0 = E[\|\mathbf{x}_k\|^2] / E[\|\mathbf{n}_k\|^2]$.

Thanks to the channel coding and subcarrier interleaving, the OFDM offers frequency diversity [16]. The frequency diversity order (i.e., the independent subcarriers) can be approximately estimated as the ratio of the system bandwidth to the coherence bandwidth of the channel. The coherence bandwidth can be readily obtained from the autocorrelation function (ACF) of the channel frequency response. In open-loop spatial multiplexing, the LTE base station (BS) employs large delay cyclic delay diversity (CDD) [16] that effectively converts spatial diversity into frequency diversity. Hence, effective (instantaneous) SNR taking the frequency diversity into account can be modeled as $\gamma = \sum_{i=1}^{N_T}\sum_{k=1}^{N_d}\gamma_i^{(k)} \Big/ N_T N_d$, where N_d is the number of independent subcarriers. The empirical CDF of γ is $F(\gamma_{th};\bar{\gamma}) = \sum_{n=1}^{N}\mathbf{1}\left\{\gamma^{(n)} \le \gamma_{th}\right\}\Big/N$, where $\mathbf{1}\{\text{A}\}$ is an indication function (that equals one if the event A is true and zero otherwise), $\gamma^{(n)}$ is the nth realization of γ, and N is the number of realizations (samples) of the random fading channel.

III. MEASUREMENTS AND SIMULATIONS

The throughput measurements are confined to 2×2 MIMO systems due to the availability of a two-port BS emulator. Specifically, the Anritsu MT8820C is used as the BS emulator; the Keysight Propsim is used as the channel emulator; and a mobile phone of Samsung Galaxy S4 is used as the device under test (DUT). For throughput measurements, the BS emulator is set for open-loop spatial multiplexing with a MCS index of 13, LTE frequency band 3, frequency-division duplex (FDD), and 10-MHz bandwidth. The DUT is located in a RF shielded box to eliminate unwanted interferences. Note that the output ports of the channel emulator are connected to the antenna ports of the DUT via two RF cables and the internal antennas of the DUT are, therefore, bypassed. The antenna patterns are included as part of the composite channel in the channel emulator for the SCME channel models. The Kronecker channel model and SCME UMi and UMa channel models are chosen in the channel emulator, respectively. In the measurements, 20000 channel samples are generated for each of the channel model. The corresponding throughput results are shown in the sequel.

Before testing the throughput model using SCME UMi and UMa models, we first resort to the simple Kronecker channel model (with zero mean Gaussian channel coefficients). We emulate uncorrelated channel (correlation = 0 at both transmit and receive side) and (almost) totally correlated channel (correlation = 0.999 at both transmit and receive side). For both cases, only one channel tap is generated so that the channel is frequency-flat and there is only one independent subcarrier.

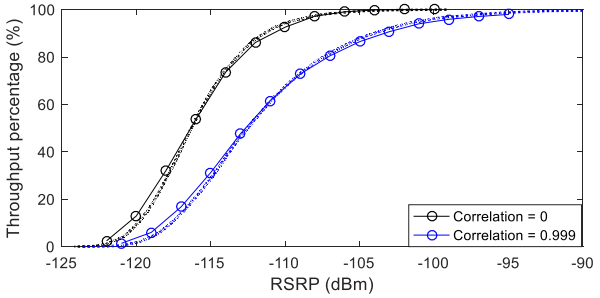

Fig. 2. Measured (solid) and simulated (dotted) throughputs of the Kronecker channel model.

Fig. 3. Photo of the mockup handset antenna.

Figure 2 shows the measured and simulated throughputs of the Kronecker channel model as a function of the reference signal received power (RSRP). The measured throughputs are shown in solid curves, whereas the simulated throughputs (using the throughput model) are shown in dotted curves. An interesting observation is that the uncorrelated channel offers higher diversity order than the totally correlated channel does (i.e., the slope of the throughput curve of the uncorrelated channel is larger than that of the totally correlated channel). This is because the large delay CDD [16] offers a diversity order of two in the uncorrelated channel, yet no diversity order for the totally correlated channel. As can be seen, the throughput model can well predict the measurements. Note that the total correlation drastically degrades the throughput performance (i.e., one needs to boost the power tremendously to be able to measure the throughput of the totally correlated channel). Unfortunately, the boosted power in the measurements was not recorded. The modeled throughput curve of the totally correlated channel has been shifted to the left by about 47 dB in the figure to match the measurement. It is expected that the same amount of power has been boosted for the totally correlated channel case. As will be shown for the throughput measurement of the SCME channel models later, the throughput model can actually predict the (power) degradation caused by the correlation as well as the branch power ratio (BPR).

In order to validate the throughput model using more realistic channel models, SCME UMi and UMa channel models [15] are selected in the channel emulator, respectively. Unlike the Kronecker channel model, BS antenna characteristics, multipath propagation channels, and mobile antenna characteristics are included in the SCME UMi and UMa channel models implemented in the channel emulator. The BS antenna consists of two $\pm 45^{o}$ tilted dipoles [1]. A mockup MIMO antenna (see Fig. 3) is selected as the mobile antenna. It consists of two planar inverted-F antennas (PIFAs) at the two ends of the mobile chassis with a separation of about 0.7λ (where λ denotes the wavelength). The dual-polarized antenna patterns are measured in an anechoic chamber and imported to the channel models. This is referred to as the two-stage method in this study.

To emulate the MPAC method, the single-polarized channel impulse response (CIR) of the *l*th path (cluster) between the *u*th antenna in the BS and the *s*th antenna in the mobile phone is expressed as [13]

$$h_{s,u,l}(t,\tau) = \sum_{p=1}^{P} f_s^{MS}(\varphi_p) h_{u,p,l}^{OTA}(t,\tau) \tag{4}$$

where t and τ denotes the time and delay, respectively, P is the number of probes, $f_s^{MS}(\varphi_p)$ denotes the complex antenna response of the pth probe to the sth mobile antenna (that is measured in an anechoic chamber for the MPAC setting),

$$h_{u,p,l}^{OTA}(t,\tau) = \sqrt{w_{p,l} g_l}\,\delta(\tau-\tau_l) \sum_{m=1}^{M} f_u^{BS}(\phi_{l,m}) e^{j\frac{2\pi}{\lambda}\cos\theta_{l,m,u}} \times e^{j(2\pi\nu_{l,m}t+\Phi_{l,m,p})} \tag{5}$$

where $w_{p,l}$ is the power weights at the pth probe for the lth path (that is obtained via convex optimization [2]), g_l and τ_l are the power and delay of the lth path, δ is the Dirac delta function, f_u^{BS} is the complex antenna pattern of the uth BS antenna, $\phi_{l,m}$, $\nu_{l,m}$, and $\Phi_{l,m,p}$ are the angle of departure, Doppler frequency, and initial phase of the mth subpath of the lth path (and of the pth probe), and $\theta_{l,m,u}$ is the angle between $\phi_{l,m}$ and the local vector of the uth BS antenna. Note that, for notational convenience and without loss of generality, only one polarization of the CIR has been expressed in (4) and (5). The dual-polarized CIR can be expressed similarly by adding a 2×2 polarization rotation matrix to account for the cross polarization ratio in the propagation channel [15]. Also note that the channels from the probes to the ports of the mockup antenna are measured beforehand and incorporated into the composite channel in the channel simulator via (4) and (5). Specifically, in this work, we assume 8 probes (P = 8) to ensure that the testing zone of the MPAC method is slightly larger than PIFA separation of the mockup antenna (0.7λ) [2].

The 10-MHz bandwidth contains 50 resource blocks (RBs), and each RB corresponds to 12 subcarriers. Hence, there are 600 (useful) subcarriers within each OFDM symbol. Both SCME UMi and UMa channel models [15] have 18 paths. In order to account for the frequency diversity order (cf. Section II), we need to estimate the number of independent subcarriers. To that end, we first transform the CIR from the delay domain into the channel frequency response (CFR) in the frequency domain. The ACF of the CFR is defined as

$$ACF_{s,u}(f,\partial f) = \frac{E\left[H_{s,u}^{*}(f,t)\cdot H_{s,u}(f+\partial f,t)\right]}{E\left[|H_{s,u}(f,t)|^{2}\right]} \tag{6}$$

where $H_{s,u}(f,t)$ is the CFR from the uth antenna in the BS to the sth antenna in the mobile phone, and the expectation is taken over the time sample. Assume that the channel is wide sense stationary, $ACF_{s,u}(\partial f) = ACF_{s,u}(f,\partial f)$.

Figure 4 shows the ACF between an arbitrary transmit-receive pair for the SCME UMi channel (generated using the two-stage method). The coherence bandwidth is 0.54 MHz. The coherence bandwidths of the CFRs between other transmit-receive pairs are similar. The coherence bandwidth of the SCME UMa channel can be obtained using the same procedure. The number of independent subcarriers is estimated as the ratio of the system bandwidth to the coherence bandwidth. There are about 18 independent subcarriers for the SCME UMi channel model and 20 independent subcarriers for the SCME UMa channel model. The independent subcarriers are (approximately) equally spaced over the 600 subcarriers.

In order to show the effect of independent subcarriers on throughput modeling, we plot the modeled throughputs using 1 subcarrier, 18 independent subcarriers, and all the 600 subcarriers, respectively, against the measured throughput using the two-stage method in Fig. 5. (Note that the modeled throughput using 18 independent subcarriers overlaps with that using all the 600 subcarriers.) As can be seen, the modeled throughput using one subcarrier clearly underestimates the diversity order and that there is little point of using more subcarriers than the independent subcarriers in modeling the throughput (given the fact that the simulation time increases with increasing number of subcarriers).

Figure 6 shows the measured and modeled throughputs using the two-stage method and the emulated MPAC method for SCME UMi and UMa models. The measured throughputs using emulated MPAC method agree well with that of the two-stage method. More importantly, it can be seen that the throughput model (using corresponding channels) can well predict the measured throughputs for SCME UMi and UMa channel models using both methods. The reasons that the throughput performance in the SCME UMa channel is worse than that in the SCME UMi channel are (a) the branch power ratio (BPR) of the former is about 4.7 dB whereas the BPR of the later is only 0.2 dB and (b) the former has very high correlation (about 0.96 at the BS and 0.66 at the mobile) whereas the later has very low correlation (below 0.1 at both sides). As can be seen, the throughput model can well predict the throughput degradation due to the BPR and correlations.

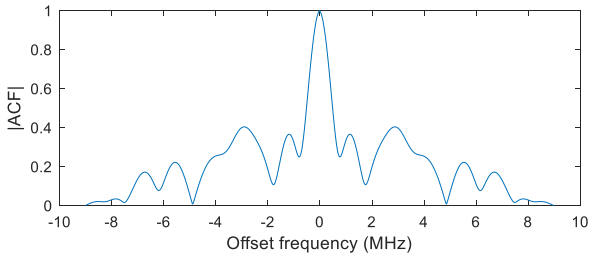

Fig. 4. Example of ACF magnitude of the SCME UMi channel generated using the two-stage method.

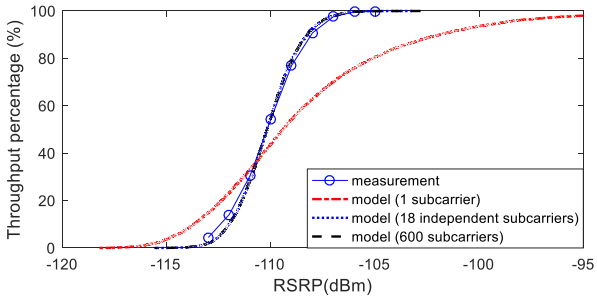

Fig. 5. Measured throughput and modeled throughputs using 1 subcarrier, 18 independent subcarriers, and all the 600 subcarriers for the SCME UMi channel generated by the two-stage method.

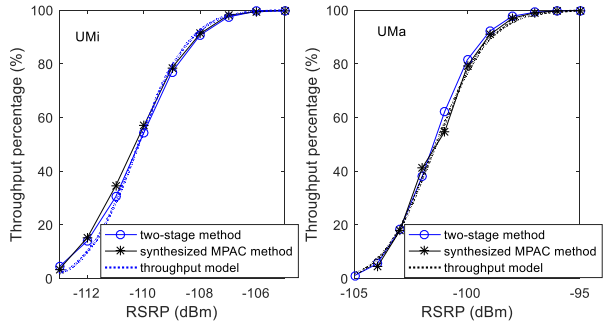

Fig. 6. Measured (solid) and modeled (dotted) throughputs using the two-stage method and the emulated MPAC method: (a) SCME UMi; (b) SCME UMa.

IV. Conclusion

In this letter, we extended the throughput model to arbitrary multipath fading channels. A channel emulator was used to generate Kronecker channel model, and SCME UMi and UMa channel models, respectively. The corresponding throughputs were measured. It was shown that, using the Kronecker model, the slope of the measured throughput curve (as a function of RSRP) reduces when the channels are totally correlated. This phenomenon can be well captured and explained by the throughput model. For throughput modeling of arbitrary multipath fading channels, it suffices to model the throughput using independent subcarriers. While modeling the throughput using more subcarriers will increase the simulation time yet yield the same result, modeling the throughput with insufficient subcarriers will underestimate diversity order (i.e., the slope of the throughput curve) of the LTE system. Finally, it was shown that the throughput model well predicts the measured throughput using either the two-stage method or the emulated MPAC method for SCME UMi and UMa channel models.

References

[1] *Test Plan for 2×2 Downlink MIMO and Transmit Diversity Over-the-Air Performance*. CTIA Certification, Tech. Rep. Version 1.1, Aug. 2016.

[2] W. Fan, X. Carreno, Fan Sun, *et al*., "Emulating Spatial Characteristics of MIMO Channels for OTA Testing," *IEEE Trans. Antennas Propag*., vol. 61, no. 8, pp. 4306-4314, Aug. 2013.

[3] D. Micheli, M. Barazzetta, F. Moglie, and V. M. Primiani, "Power boosting and compensation during OTA testing of a real 4G LTE base station in reverberation chamber," *IEEE Trans. Electromagn. Compat.*, vol. 57, no. 4, pp. 623–634, Aug. 2015.

[4] W. Yu, Y. Qi, K. Liu, *et al.*, "Radiated two-stage method for LTE MIMO user equipment performance evaluation," *IEEE Trans. Electromagn. Compat.*, vol. 56, no. 6, pp. 1691–1696, Dec. 2014.

[5] P.-S. Kildal, A. Hussain, X. Chen, *et al*., "Threshold receiver model for throughput of wireless devices with MIMO and frequency diversity measured in reverberation chamber," *IEEE Antennas Wireless Propag. Lett*., vol. 10, pp. 1201-1204, 2011.

[6] X. Chen, "Throughput modeling and measurement in an isotropic-scattering reverberation chamber," *IEEE Trans. Antennas Propag.*, vol. 62, no. 4, pp. 2130-2139, Apr. 2014.

[7] *Harmonization analysis*. Intel Corporation, CATR, 3GPP TSG-RAN WG4 Meeting #83, Hangzhou, China, May 15 – 19, 2017.

[8] D. Micheli, M. Barazzetta, C. Carlini, *et al*., "Testing of the carrier aggregation mode for a live lte base station in reverberation chamber," *IEEE Trans. Veh. Technol.*, vol. 66, no. 4, pp. 3024-3033, Apr. 2017.

[9] Q. Xu, Y. Huang, X. Zhu, *et al.*, "A new antenna diversity gain measurement method using a reverberation chamber," *IEEE Antennas Wireless Propag. Lett.*, vol. 14, pp. 935 - 938, 2015.

[10] M. Barazzetta, D. Micheli, L. Bastianelli, *et al*., "A comparison between different reception diversity schemes of a 4G-LTE base station in reverberation chamber: a deployment in a live cellular network," *IEEE Trans. Electromagn. Compat.*, vol. 59, no. 6, pp. 2029–2037, Dec. 2017.

[11] A. Paulraj, R. Nabar and D. Gore, *Introduction to Space-Time Wireless Communication*, Cambridge University Press, 2003.

[12] Y. Jing, H. Kong, and M. Rumney, "MIMO OTA test for a mobile station performance evaluation," *IEEE Instrument. Meas. Mag.*, vol. 19, no. 3, pp. 43–50, Jun. 2016.

[13] W. Fan, L. Hentilä, P. Kyösti, and G. F. Pedersen, "Test zone size characterization with measured MIMO throughput for simulated MPAC configurations in conductive setups," *IEEE Trans. Veh. Technol.*, vol. 66, no. 11, pp. 10532-10536, Nov. 2017.

[14] M. R. D. Rodrigues, I. Chatzigeorgiou, I. J. Wassell, and R. Carrasco, "Performance analysis of turbo codes in quasi-static fading channels," *IET Commun.*, vol. 2, no. 3, pp. 449–461, 2008.

[15] *Spatial channel model for Multiple Input Multiple Output (MIMO) simulations*. 3rd Generation Partnership Project Tech. Rep. 3GPP TR 25.996 V13.0.0, Dec. 2015.

[16] *LTE; Evolved Universal Terrestrial Radio Access (E-UTRA); Physical channels and modulation*. 3rd Generation Partnership Project, TS 36.211 version 11.2.0 Release 11, Apr. 2013.